Pergamon

SCIENCE DIRECT®

Bioorganic & Medicinal Chemistry 11 (2003) 1269–1281

BIOORGANIC & MEDICINAL CHEMISTRY

Novel B-Ring Modified Allocolchicinoids of the NCME Series: Design, Synthesis, Antimicrotubule Activity and Cytotoxicity

Silke Bergemann,[c] René Brecht,[a] Frank Büttner,[a] Daniel Guénard,[b] Ronald Gust,[c] Gunther Seitz,[a,*] Milton T. Stubbs[a] and Sylviane Thoret[b]

[a]*Pharmazeutisch-Chemisches Institut der Philipps-Universität, Marbacher Weg 6, D-35032 Marburg, Germany*
[b]*Institut de Chimie des Substances Naturelles, Centre National de la Recherche Scientifique, Avenue de la Terrasse, 91198 Gif-Sur-Yvette Cedex, France*
[c]*Institut für Pharmazie I der Freien Universität Berlin, Königin-Luise-Str. 2 u. 4, D-14195 Berlin, Germany*

Received 28 August 2002; accepted 29 November 2002

Abstract—Two new series of allocolchicinoids mimicking the structure of (−)-*N*-acetylcolchinol *O*-methyl ether (**2**, NCME) were synthesized and evaluated for their abilities to inhibit tubulin assembly. Possible antitumor properties resulting thereof were evaluated in vitro on the human MCF-7 breast cancer cell line. The first series of NCME-derivatives was brought about by extending the seven membered B-ring to novel semisynthetic variations with a nitrogen containing *eight-membered* B-ring similar, for example, to the artificial, potent steganacin aza-analogue **3**. In the second series the seven-membered B-ring of NCME (**2**) was modified by annulation with a heterocyclic ring system. The racemic ketone **7a** serving as key precursor involved in the syntheses of all the target NCME variants **9**–**13** and **15**, **16** was easily transformed into the eight-membered B-ring lactams **9** and **10** via a Beckmann rearrangement of the corresponding *E*-oxime **8**. The tetrazole annulated congener **11** was prepared via azidotrimethylsilane-mediated Schmidt rearrangement. Treatment of educt **7a** with Bredereck's reagent led to the enamino ketone **14**, which was easily converted into the pyrazole- or pyrimidine-annulated allocolchicinoids **15** and **16**. Remarkably, all the allocolchicinoids **9**–**13** with an azocin-B-ring affected the tubulin/microtubule equilibrium only moderately. In contrast, the novel heterocycle annulated seven membered B-ring variants **15** and **16** proved to be highly potent tubulin-inhibitory, antimitotic agents. Interaction with tubulin occured at concentrations similar to those observed for colchicine (**1**) or the lead NCME (**2**). In all cases the antiproliferative effects correlated roughly with the inhibition of tubulin assembly.

Introduction

In continuation of our efforts[1] directed towards the development of hitherto unknown B-ring modified allocolchicinoids,[2–7] we have focused our attention on the syntheses of novel variants of the highly potent (−)-*N*-acetylcolchinol *O*-methyl ether (**2**, NCME).[8] This synthetic antitubulin agent **2** is a member of the allo series of native (−)-(*aR,7S*)-colchicine (**1**) with a benzenoid rather than a tropolone C ring, as occurs in the natural alkaloid **1**. Both proved to be effective antimitotic agents as important representatives of inhibitors of the tubulin-microtubule equilibrium.[3,9] Compared to the parent alkaloid **1** the allocolchicinoid NCME (**2**) combines a higher affinity for tubulin with a better stability and thus served as a standard by which antitubulin activity in vitro can be measured.[9] Like (−)-(*aR,7S*)-colchicine (**1**) NCME (**2**) is characterized by an atropisomeric biaryl unit[10]—comprising a trimethoxyphenyl ring connected with a *p*-oxymethyl substituted benzene unit. Due to the helicity of the sigma-bond joining these two phenyl moieties allocolchicinoid **2** is an axially chiral species additionally endowed with a chiral center at C-7 (atom numbering referring to **1**). An X-ray analysis of an urea-derivative of compound **2** was used for the indirect assignment of the absolute configuration of C-7 and of the biphenyl unit to be (*aR,7S*) in the crystal. Thus, NCME (**2**) is equipped with the proper stereochemical arrangement of the A–C biphenyl backbone, a requirement for the interaction with tubulin.[11] As indicated by NMR studies NCME (**2**) exists in solution as an atropisomeric mixture of (*aR,7S*)/(*aS,7S*) isomers. The (*aR*)/(*aS*) equilibrium dominated by the configurationally unstable (*aR*)-conformer varies with

*Corresponding author. Tel.: +49-6421-282-5809; fax: +49-6421-282-6652; e-mail: seitzg@mailer.uni-marburg.de

0968-0896/03/$ - see front matter © 2003 Elsevier Science Ltd. All rights reserved.
doi:10.1016/S0968-0896(02)00639-9

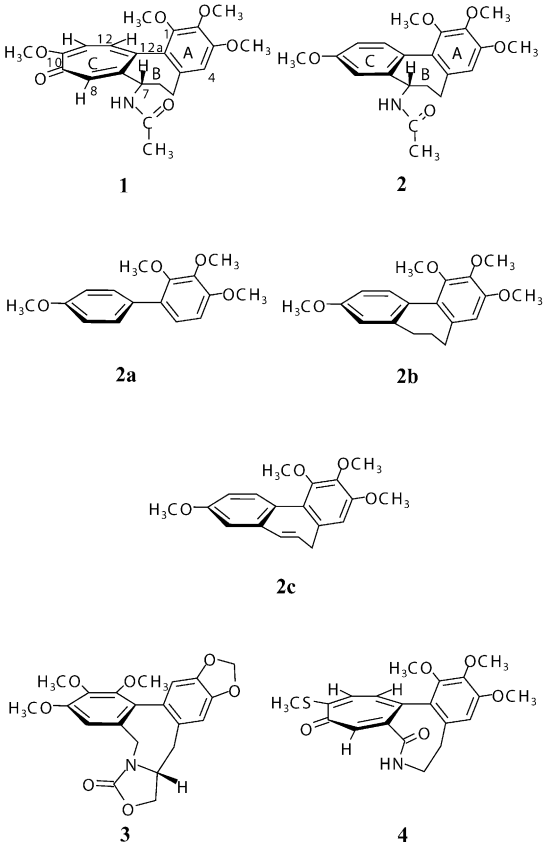

Scheme 1. (−)-(*aR,7S*)-Colchicine (**1**), allocolchicinoid (−)-(*aR,7S*)-NCME (**2**), NCME-variants **2a–c**, steganacin aza-analogue **3** and (*aR*)-thiocolchicinoid **4**.

solvent and temperature. Additionally, the biaryl moiety is linked by a three-atom-bridge (thus also referred to as an *o,o′*-bridged biphenyl) giving rise to a bis(benzocycloheptadiene) skeleton (Scheme 1).

It is well accepted that the *primary* pharmacophore of NCME (**2**) consists of the A and C rings, the character of the B-ring however decisively contributes to the efficacy of the antimicrotubule agent especially by influencing the conformational mobility of the A–C biphenyl backbone upon tubulin binding. Removal of the B-ring of NCME (**2**) leading to TMB (**2a,** 2,3,4,4′-tetramethoxy-1,1′-biphenyl) decreases the affinity of the allocolchicinoid for tubulin.[7] The loss of activity (in the absence of the tethering B ring) however, is attributed to the *conformational* properties of TMB (**2a**) and not directly to binding site interactions.[12]

With this in mind, we focused our interest on two attractive modifications of NCME (**2**). On the one hand, this was brought about by extending the seven-membered B-ring to novel semisynthetic variations such as **9–13** characterized by a central azocin-ring (Scheme 2). These species additionally mimic the structures of the artificial, potent steganacin aza-analogue **3**[13] or the thiocolchicinoid **4**[14] (Scheme 1) comprising an eight membered B-ring lactam. On the other hand, we were interested in modifying the seven membered B-ring of NCME (**2**) by annulation with a heterocyclic ring system as realized in the ligands **15** and **16** (Scheme 3).

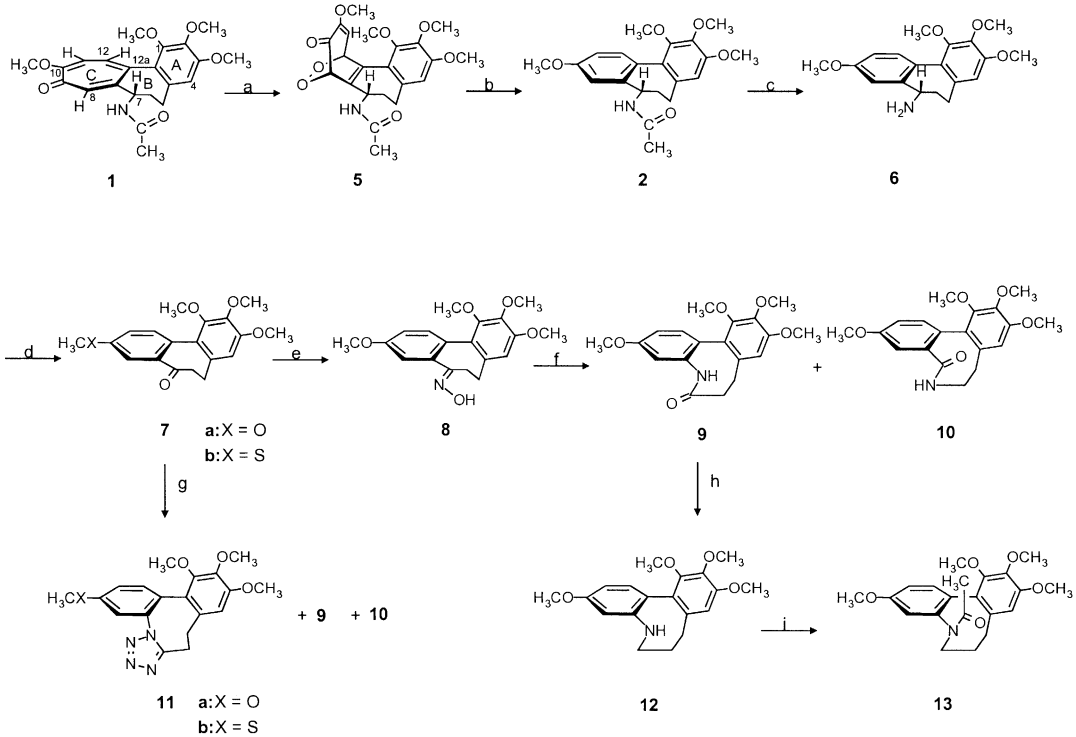

Scheme 2. Reagents and conditions: (a) $^1O_2$, hν, hematoporphyrin, $CHCl_3$, 80%; (b) Ph_3P, CH_2Cl_2, rt, 40% from **1**; (c) 2 M aqueous hydrochloric acid, CH_3OH, 20 h reflux, 75%; (d) FMPB/DMF/ CH_2Cl_2, DBN, $(CO_2H)_2/H_2O$, 67%; (e) $NH_2OH{\cdot}HCl$, Na_2CO_3, CH_3OH (92%), reflux 24 h, 91%; (f) PPA, 70 °C, 20 h, 65% and 7%, resp.; (g) $(H_3C)_3SiN_3$, CF_3CO_2H, rt, 24 h, 68% (besides 13% of **9** and 5% of **10**); (h) $LiAlH_4$, THF, Pyridin, 24 h, 55% (besides 30% of **9**); (i) pentafluorophenylacetate, DMF, 80 °C, 20 h, 85% (concerning the atomic numbering used see Experimental).

Both of these structural variations [with all the methoxy groups similarly positioned as in NCME (**2**)] are anticipated to modify the inter-ring torsional angle between the A and C moieties of the biaryl backbone and consequently the binding properties to tubulin. Fortunately, NCME (**2**) is easily accessible[8] by photooxygenation of the parent alkaloid **1** with singlet oxygen in the presence of hematoporphyrin—an application of methodology developed in these laboratories—providing primarily the endoperoxide **5**. This intermediate could successfully be transformed into NCME (**2**) in fair yield by treatment with $(Ph)_3P$ in dichloromethane at room temperature. Syntheses and spectroscopic data of these novel B-ring modified allocolchicinoids are described together with an evaluation of their abilities to inhibit the assembly of tubulin and the growth of the human MCF-7 breast cancer cell line.

Chemistry

A particularly attractive synthetic route to gain novel B-ring variations of NCME (**2**) originates from the ready transformation of allocolchicinoid **2** into the well-known ketone **7a** (Scheme 2)—the synthesis of which was realized through the application of novel extensions to existing methodology employed in these laboratories[15] and independently by Lee et al.[16] Thus, the acetamido group of NCME (**2**) was subjected to acidolysis with methanolic hydrochloric acid to form the deacetylated allocolchicinoid colchinol-*O*-methylether (**6**, COME). Biomimetic transamination of COME (**6**) using 4-formyl-*N*-methyl-pyridinium benzenesulfonate (FMPB) led in high yield to the requisite ketone **7a** which was isolated as racemic mixture. Obviously its two enantiomers with a chiral biphenyl backbone are configurationally unstable. A rapid atropisomerism occurs due to a low energetical barrier to rotation around the central biaryl bond. The ketone **7a** served as key precursor involved in the syntheses of the target allocolchicinoids **9**, **10**, **11a**, **12**, **13**, **15** and **16**. Treatment of the ketone **7a** with hydroxylamine hydrochloride/sodium carbonate[17] afforded the corresponding *E*-oxime **8** (*anti*), most strikingly, as the sole isolated product.

The *E*-structure of **8** was unambiguously verified by X-ray crystallographic analysis (see Experimental). An ORTEP plot of the solid state conformation of the *E*-(*aR*)-atropisomer of **8** is presented in Figure 1.

Utilizing Berg's methodology[14] for the Beckmann rearrangement the oxime **8** was transformed into a mixture of the two lactams **9** and **10.** Because of the preferential migration of the group *anti* to the oxime hydroxyl group, the isomer **9** dominated as expected in a ratio 10:1. Probably, a small amount of the *E*-oxime undergoes isomerisation under the reaction conditions *before* migration takes place. Both products **9** and **10** could easily be separated by careful column chromatography. Reduction of the lactam group of allocolchicinoid **9** with $LiAlH_4$ led to the unstable dibenz[*b*,*d*]azocine **12**, which was quickly transformed (without full characterization) into the acetamide **13** by treatment with pentafluorophenylacetate.[18,19] The novel allocolchicinoid **13** was identified by its spectroscopic properties and additionally verified by an X-ray crystallographic analysis as detailed in the Experimental. A perspective view (ORTEP) of the solid-state structure of the (*aR*)-atropisomer of the racemic allocolchicinoid **13** is presented in Figure 2.

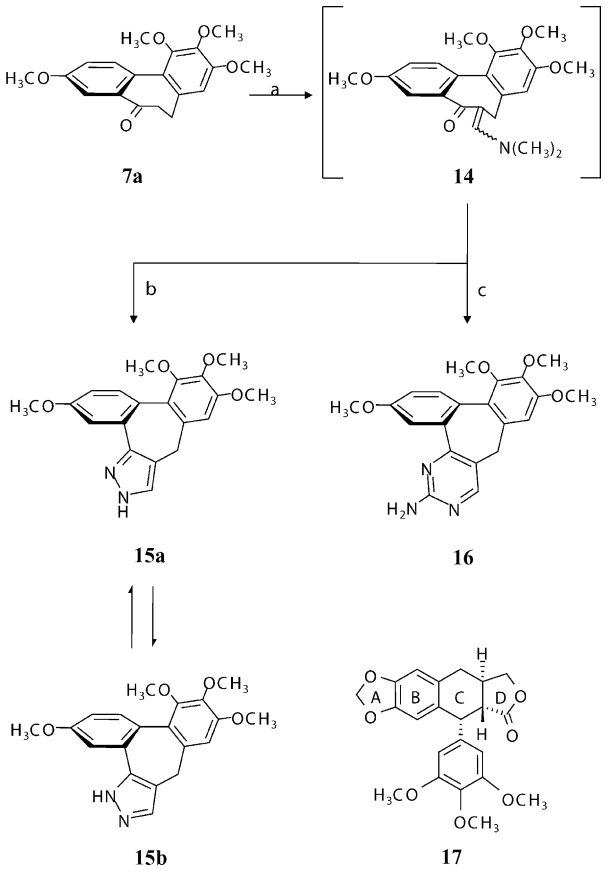

Scheme 3. Reagents and conditions: (a) Bredereck's reagent, DMF, 60 °C, 24 h; (b) NH_2–NH_2·2HCl, CH_3OH, rt, 24 h; 58%; (c) C_2H_5ONa, guanidine·HCl, C_2H_5OH, reflux, 3.5 h, 96%.

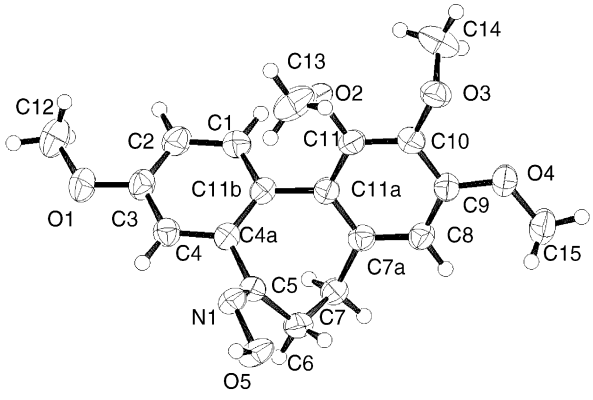

Figure 1. Structure of the oxime **8** determined by X-ray crystallography. ORTEP diagram (50% probability ellipsoids) showing the crystallographic atom-numbering scheme and solid-state conformation of the *E*-(*aR*)-enantiomer in crystals of the racemic oxime **8**; small circles represent hydrogen atoms.

In order to gain satisfying amounts of the minor lactam **10** we investigated the azidotrimethylsilane- (TMSA) mediated Schmidt rearrangement[20] of ketone **7a** expecting a more non-regioselective carbon migration (i.e., alkyl over aryl migration). However, under the reaction conditions employed the substrate **7a** afforded the lactams **9** and **10** in very low yield of 13% and 5%, respectively. Main product with 68% yield was the tetrazole fused allocolchicinoid **11a** the structure of which could be determined by spectroscopic methods and additionally by X-ray diffraction analysis (Fig. 3).

Application of the same protocol with the ketone **7b**[21] as starting material afforded the corresponding tetrazole fused allocolchicinoid **11b** with a yield of 46%.

The second intention of this project to prepare novel NCME-type allocolchicinoids with a seven membered B-ring modified by annulation with a heterocyclic ring system could be realized, too, with ketone **7a** as starting material. This could efficiently be transformed into the pyrazole fused allocolchicinoid **15** (to be composed of the tautomers **15a/15b**) in two steps as outlined in Scheme 3. Treatment of the starting ketone **7a** with Bredereck's reagent [bis(dimethylamino)-*tert*-butoxymethane][22,23] provided the enamino ketone **14** the key intermediate for the synthesis of the target compounds **15** and **16**. This was simply converted on reaction with hydrazine dihydrochloride[24] into mixtures of the pyrazoles **15a/15b** with 58% yield. With regard to the NMR timetable there is a fast proton-transfer between the two pyrazole-N-atoms of **15** which increases the symmetry of the system.[25] Thus, it was not possible to observe both isomers in the ^{1}H and ^{13}C NMR spectra as it is expected for tautomers. The spectra of **15a**/**15b** gave mean absorption values. Because of the transfer processes the involved ^{13}C-signals showed a significant broadening of the lines and all the signals of the quaternary carbons of the pyrazole moieties could not be detected at 25 °C. Elaboration to the 2-aminopyrimidine annulated allocolchicinoid **16** proceeded by condensation of the enamino ketone **14** with guanidine hydrochloride in the presence of sodium ethanolate in ethanol using a previously established protocol[26] providing the target compound in 96% yield.

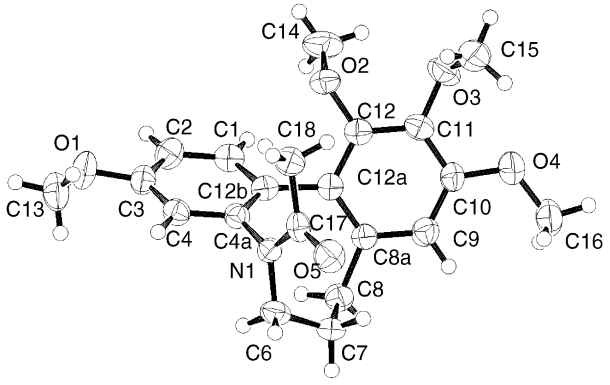

Figure 2. ORTEP diagram (50% probability ellipsoids) showing the solid-state conformation of the (*aR*)-atropisomer of the racemic allocolchicinoid **13** (with numbering through the text).

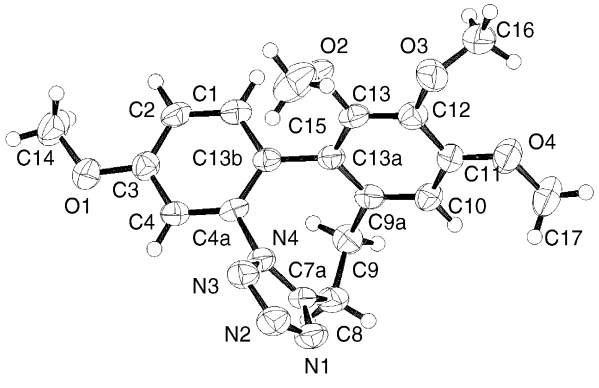

Figure 3. ORTEP diagram (50% probability ellipsoids) showing the solid-state conformation of the (aR)-atropisomer of the racemic tetrazole fused allocolchicinoid **11a** (with numbering through the text).

Biological Results and Discussion

In vitro tubulin binding assay

All of the newly synthesized allocolchicinoids **8**–**11**, **13**, **15a**/**15b** and **16** were subjected to our standard assay conditions[1,27,28] for evaluation of tubulin assembly inhibition in vitro using calf brain tubulin. In order to allow a precise comparison between the novel ligands and the lead NCME (**2**), the well-known allocolchicinoids COME (**6**) and ketone **7a** were included in the evaluation. The IC_{50} values of all the allocolchicinoids under consideration were compared to that of deoxypodophyllotoxine (DPPT, **17**) as the standard, measured within the same day with the same tubulin preparation. The data are compiled in Table 1, presented in terms of the relative IC_{50}/IC_{50DPPT} value determined from the IC_{50} values of the test compounds.

As can be seen from the data listed in Table 1 NCME (**2**) equals the standard DPPT (**17**) in its inhibitory effect. *N*-Deacetylation of NCME (**2**) exhibited an unexpected negative impact on the activity as antimitotic agent. COME (**6**) proved to be 25 times less active in comparison with DPPT (**17**) and NCME (**2**). Among the allocolchicinoids newly synthesized and

Table 1. Inhibition of in vitro tubulin assembly

Compound	$IC_{50}/IC_{50\ DPPT}$
Colchicine (**1**)	4–8
NCME (**2**)	1
COME (**6**)	25
7a	1.3
8	1.0
9	63
10	Inactive
11a	7
11b	6
13	7
15a/15b	1.4
16	2
DPPT (**17**)	1.0[a]

[a]$IC_{50\ DPPT}$ varies from 1.0 to 3.0 μM for the different experiments according to the tubulin concentration.

tested none of them exhibited a higher activity than DPPT (**17**). The ketoxime **8** turned out as the most active inhibitor of the tubulin/microtubule equilibrium by binding to the colchicine site. It equaled DPPT (**17**) as well as the lead NCME (**2**) and slightly surpasses the inhibitory effect of the corresponding ketone **7a** and that of the dihydro-tetramethoxy-dibenzo[*a*,*c*]cycloheptene **2b**.[29] The solid state conformation and the stereochemistry of ligand **8** were determined using single-crystal X-ray diffraction techniques (Fig. 1). An advantage of having available the crystal structure of this ligand was the possibility to obtain detailed information of the three-dimensional arrangement. It is beneficial for defining the exact stereochemistry of oxime **8**, for example for the determination of the *E*-oxime configuration (anti) and to settle the possible range of conformational variation among the allocolchicinoids under consideration, for example concerning the torsional angle between the least-squares of the two aromatic A- and C-rings, accepted as the most definitive conformational attribute.[15] In the case of oxime **8** this turned out to be 53°, just like in (−)-(*aR,7S*)-colchicine (**1**) or in other highly potent allocolchicinoids.[11] The significant inhibitory effect of the racemic ligand **8** is so much the more remarkable as compared to the enantiopure NCME (**2**) only 50% of the ligand possesses the appropriate helicity requisite for tubulin binding.

The novel NCME-type allocolchicinoids in the series with an azocin-B-ring **9**–**13** displayed remarkably different ability to inhibit tubulin assembly obviously attributed to different conformational properties of these ligands.[12] All of them are devoid of the stereogenic center C-7 of NCME (**2**) and exist as racemic mixtures of two enantiomeric conformations due to hindered rotation around the pivot bond joining the A and C rings which are twisted by noteworthyly different torsional angles. Surprisingly, the structurally different azacyclooctanoids **9** and **10** do not notably affect tubulin assembly despite structural similarity of, for example, **10** especially with the thiocolchicinoid **4**.[14] This is consistent with earlier findings in the androbiphenyline series[1] and probably due to different conformational properties compared to NCME (**2**) with a dibenzo[*a*,*c*]-cycloheptadiene skeleton. As molecular models reveal the change from a three- to a four-atoms bridge linking the A–C biaryl backbone in the lactams **9** and **10** results in comparatively rigid molecules with stable conformations. It comprises a significant increase of the torsional angle between the planes of the A- and C-ring from ca. 53° in highly potent anti-tubulin agents such as NCME (**2**) to more than 75° in ligands with an azocin-B-ring lactam.[14] Obviously the tubulin binding site seemed to be unable to accommodate such ligands. These results underline the importance of the B-ring to influence the conformational properties of the A–C biaryl backbone of an allocolchicinoid and thus the antimicrotubule activity.

Introduction of an annulated tetrazole moiety instead of the lactam group (**9** and **10**) leads to the allocolchicinoids **11a** and **11b** and contributes positively to the inhibition of tubulin assembly. Conformational variation in these tetracyclic allocolchicinoids due to the extra strain introduced into the molecules by the tetrazole ring is obviously connected with a 10-fold higher antimicrotuble activity as compared to the lactam **9**, although 6-fold less potent relative to the lead NCME (**2**). Judging from the X-ray structure of ligand **11a** (Fig. 3) exhibiting the A- and C-rings tilted with respect to the pivot-bond and a torsional angle between the least-squares planes of the A–C biaryl backbone of ca. 58° the observed antitubulin activity of the allocolchicinoid **11a** with a relative IC_{50}/IC_{50DPPT} value of 6 was not unexpected. Structurally related to the only weakly potent NCME-variant **9** with an azocin-B-ring lactam is the *N*-acetylated dibenzo[*b*,*d*]azocin **13**, characterized by a solid-state conformation with a torsional angle between the least-squares planes of the A–C biaryl unit of 59° (Fig. 2). Similar to ligand **11a** the overall structural conformation of the azacyclooctanoid **13** is less twisted probably due to the at least in the crystal energetically favored axially oriented *N*-acetyl group capable of decreasing the torsional angle (compared to lactame **9**) and thus leading to at least moderate antitubulin activity with a relative IC_{50}/IC_{50DPPT} value of 7.

A novel approach to systematic variations in the torsional angle between the A- and C-rings of NCME-type allocolchicinoids led to hitherto unknown heterocycle annulated tubulin ligands such as **15a/15b** and **16**. In contrast to the already mentioned tetracyclic allocolchicinoids **11a** and **11b** these are characterized by a dibenzocycloheptene scaffold as in the potent antitubulin agent **2c**,[29] which equals (−)-(*aR,7S*)-colchicine in its inhibitory effect on tubulin assembly.

In order to explore the impact of this annulation of the central B-ring of NCME-type allocolchicinoids on the tubulin-binding affinity, the ability to inhibit microtubule assembly of these pyrazole- or pyrimidine-fused NCME-variants was evaluated.

The data listed in Table 1 reveal that both species had significant inhibitory effects in this assay. Ligand **15** being slightly more potent than **16**, both surpassing the inhibitory effect of the lead (−)-(*aR,7S*)-colchicine, and the olefinic allocolchicinoid **2c**.

In vitro cell growth inhibition assay

The testing of (−)-(*aR,7S*)-colchicine (**1**) and the eight allocolchicinoids was performed on the human MCF-7 breast cancer cell line. For the evaluation of the sensitivity of this cell line against the leads **1** and **2** and the newly synthesized allocolchicinoids a computerized, kinetic chemosensitivity assay was used based on quantification of biomass by staining cells with crystal violet (see Experimental). The relationship between growth kinetics of the inhibitor-treated cell line, and the plot of corrected T/C values versus time of inhibitor cell contact (icc) were recorded as described in ref 30. In order to yield detailed insights into the mode of action, for example the inhibition profile reflecting cytostatic, transient cytotoxic or cytocidal inhibitor effects as well as development of resistance, the overall effects are

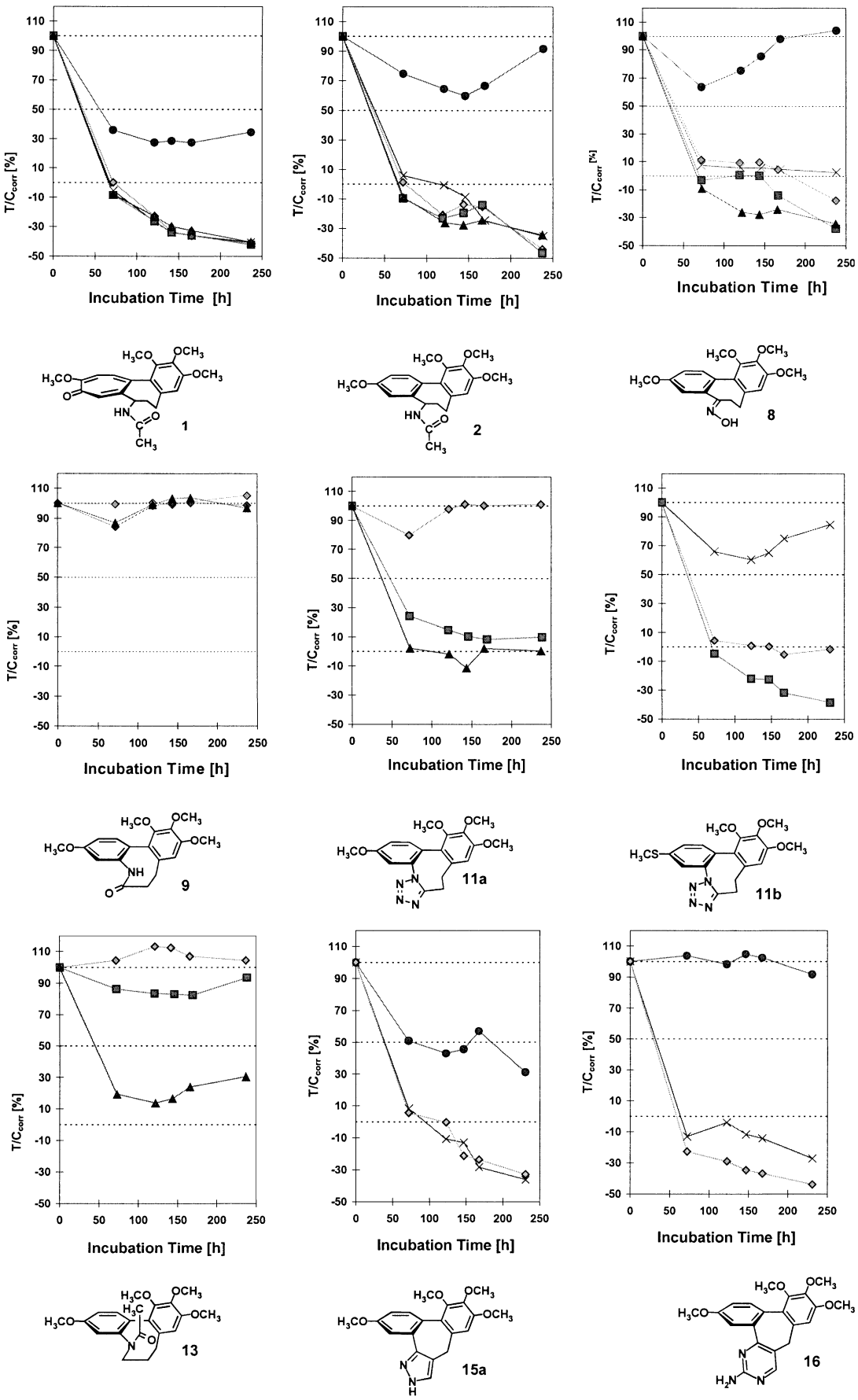

Figure 4. Effect of (−)-(*aR,7S*)-colchicine (**1**), NCME (**2**), and 7 NCME-type allocolchicinoids on the MCF-7 breast cancer cell line at concentrations: ●, 0.01 μM; ×, 0.05 μM; ◆, 0.1 μM; ■, 0.5 μM; ▲, 1 μM.

presented as plots of corrected T/C values versus icc (Fig. 4). The test details are described in the Experimental.

In Figure 4, the antitumor effects of the novel allocolchicinoids **9**–**11**, **13**, **15a/15b** and **16** were compared with those of the leads (−)-(*aR,7S*)-colchicine (**1**) and NCME (**2**). Proliferation of the MCF-7 cells was significantly inhibited by the natural alkaloid **1** even at the lowest concentration of 0.01 μM (%T/C_{corr}) causing a non transient ca. 70% growth inhibition after ca. 70 h. Concentration of 0.05 μM of the drug totally inhibited the proliferation after ca. 70 h. Comparable growth inhibition although slightly weaker and at the concentration of 0.01 μM with a transient reduction of the cell mass, was achieved with NCME (**2**) and similarly with the oxime **8**. Among the allocolchicinoids with an eight-membered azozine B-ring, lactam **9** proved to be not active even at the highest concentration of 1 μM (T/C_{corr} = 90% after 75 h icc). A significant sensitivity of the MCF-7 cells against allocolchicinoid **13** was observed only at the highest applied concentration of 1 μM (T/C_{corr} = 15% after 125 h icc, slightly transient after > 200 h). Remarkably different inhibitor effects are found with the two tetrazole annulated azacyclooctanoids **11a** and **11b**. Allocolchicinoid **11a** inhibited the growth of MCF-7 cells to the extent of 90% at concentrations of 0.5 μM (T/C_{corr} = 10% after 150 h icc) and of 100% at concentrations of 1 μM. Switch to the corresponding 3-methylthio analogue **11b** caused a 10-fold higher activity. Thus total inhibition was accomplished at concentration of 0.1 μM (T/C_{corr} = 0% after 75 h icc, cytostatic effect), whereas at a concentration of 0.5 μM a cytocidal effect was observed (T/C_{corr} = −20% after 125 h icc). Remarkable is the mode of action of the pyrazole-annulated allocolchicinoid **15a**/**15b**, which besides lead **1** proved to be the most active representative among the inhibitors tested in the MCF-7 cell culture. At a concentration of 0.01 μM compound **15a**/**15b** caused a non transient growth inhibition (T/C_{corr} = 35% after 230 h icc), while higher concentrations led to cytocidal effects (e.g., at a concentration of 0.05 μM: T/C_{corr} = −30% after 230 h icc) comparable to the effect of the leads **1** and **2**. Comparatively, the pyrimidine analogue **16** proved to be somewhat less active obvious from the weaker effects at the 0.01 μM concentration (T/C_{corr} = 90% after 230 h icc). The cytocidal effects at higher concentration are similar to those of allocolchicinoid **15a/15b**. Conclusively, the studies on the cytotoxicity of (−)-(*aR,7S*)-colchicine (**1**) and the various allocolchicinoids on the MCF-7 cell line revealed the following order of activity: **1** > **15a/15b** > **2** > **16/8** > **11b** > **11a** > **13** > > **9**.

Conclusions

We have disclosed herein the syntheses of two series of novel NCME (**2**) variants in which the seven membered B-ring of the lead **2** is extended to an azacyclooctanoid as in the allocolchicinoids **9**–**13** or annulated with a *N*-containing heterocycle as in the tubulin ligands **15** and **16**. An investigation of the biological activities led to the observation, that B-ring expansion more or less dramatically decreases the antitubulin activity, among other things mainly due to an increase of the inter-ring torsional angle between the A–C biaryl backbone, verified by crystal structure determination of the allocolchicinoids **11a** and **13**. The modest activity of the azacyclooctanoids in the tubulin test was further corroborated by low cellular toxicity. In contrast, the heterocycle fused allocolchicinoids, especially ligand **15**, resembles the leads (−)-(*aR,7S*)-colchicine (**1**) and NCME (**2**) in their tubulin assembly inhibitor potency and displays remarkable growth inhibitory activity against the human MCF-7 cancer cell line. In all cases allocolchicinoid growth inhibition correlated roughly with inhibition of tubulin assembly. Further work is needed to define more detailed SARs of the NCME series.

Experimental

General procedures

Standard vacuum techniques were used in handling of air sensitive materials. Melting points are uncorrected: 'Leitz-Heiztischmikroskop' HM-Lux. Solvents were dried and freshly distilled before use according to literature procedures. IR: FT-IR spectrometer 510-P (Nicolet). Liquids were run as films, solids as KBr pellets. ^{1}H NMR and ^{13}C NMR: Jeol JNM-GX 400 and LA 500; δ/ppm = 0 for tetramethylsilane, 7.24 for chloroform. MS: Vacuum Generators 7070 (70 eV; ^{11}B). Column chromatography: Purifications were carried out on Merck silica gel 40 (40–60 mesh), flash chromatography. Reactions were monitored by thin-layer chromatography (TLC) by using plates of silica gel (0.063–0.200 mm, Merck) or silicagel-60F_{254} microcards (Riedel de Haen). Optical rotations: Mod. Dip-370 polarimeter (Jasco). UV: Spekol UV/VIS (Jena Analytik AG).

(*E*)-6,7-Dihydro-3,9,10,11-tetramethoxy-5*H*-dibenzo[*a,c*]-cyclohepten-5-one-oxime (8).[17] To a suspension of 782 mg (2.38 mmol) of the ketone **7a**[15,16] in 50 mL of methanol (92%) were added 186 mg (2.7 mmol) of hydroxylamine hydrochloride and 95 mg (0.9 mmol) of sodium carbonate. The mixture was refluxed for 24 h and after cooling to room temperature 10 mL of water and 10 mL of chloroform were added. The phases were separated and the water phase was extracted three times with 10 mL of chloroform. The combined organic phases were dried (Na_2SO_4) and concentrated. Column chromatography (silica gel, CH_2Cl_2/MeOH 9.8:0.2) yielded 741 mg (2.16 mmol) of the oxime and 64 mg (0.19 mmol) of ketone **7a**. The oxime **8** was recrystallized from methanol to afford colorless crystals, yield 91%, mp 180 °C. UV ($CHCl_3$): λ_{max} (lgε) 228 nm (4.56), 270 (4.32). IR (KBr): ν (cm^{-1}) 3600–3100 (OH), 2939 (CH), 1597 (C=N). ^{1}H NMR (400 MHz, DMSO-d_6) δ 2.45–2.75 (m, 3H, 5-H, 6-H), 3.06 (m, 1H, 6-H), 3.46 (s, 3H, OCH_3), 3.74 (s, 3H, OCH_3), 3.80 (s, 3H, OCH_3), 3.81 (s, 3H, OCH_3), 6.75 (s, 1H, 8-H), 6.87 (d, ^4J = 2.7 Hz, 1H, 4-H), 7.01 (dd, ^3J = 8.5 Hz, ^4J = 2.9 Hz, 1H, 2-H), 7.33 (d, ^3J = 8.5 Hz, 1H, 1-H), 10.94 (s, 1H,

O*H*), ^{13}C NMR (100.5 MHz, DMSO-d_6) δ 29.2 (CH_2, C-7), 34.3 (CH_2, C-6), 54.9 (O*C*H$_3$), 55.7 (O*C*H$_3$), 60.2 (O*C*H$_3$), 60.2 (O*C*H$_3$), 107.7 (CH, C-8), 113.5 (CH, C-2*), 113.8 (CH, C-4*), 123.8 (C-11a), 126.7 (C-11b), 131.6 (CH, C-1), 135.9 (C-4a), 136.6 (C-7a*), 140.6 (C-10), 150.7 (C-11*), 152.1 (C-9*), 157.7 (C-5*), 158.4 (C-3*). *Assignments not confirmed. MS (70 eV) *m*/*z* (%): 343 (100, M^+), 327 (17). HRMS calcd for $C_{19}H_{21}NO_5$: 343.1416, found: 343.1419. $C_{19}H_{21}NO_5$ (343.38): calcd: C 66.46, H 6.16, N 4.08; found: C 66.14, H 6.19, N 4.01.

Crystal structure determination of 8

To gain single crystals of **8** for X-ray analysis, 7 mg of the oxime **8** were dissolved in CH_2Cl_2 (0.5 mL) and *n*-hexane (3 mL) was layered carefully down the side of the tube on to the solution. The tube was then corked and left to stand undisturbed for 24 h furnishing colourless crystals suitable for X-ray crystallographic analysis. A crystal of compound **8** having approximate dimension of 0.62 × 0.21 × 0.26 mm was mounted on a glass fiber and investigated on a Rigaku AFC5R diffractometer with graphite monochromated CuKα radiation and a rotating anode generator (Rigaku). Empirical formula $C_{19}H_{21}NO_5$, molecular mass 343.38 au. Cell constants and an orientation matrix for data collection, obtained from a least-squares refinement using the setting angles of 25 carefully centered reflections in the range $67.81 < 2\Theta < 79.27°$ corresponded to a primitive triclinic cell with dimensions: $a = 9.327(2)$ Å, $\alpha = 109.16(2)°$; $b = 12.524(2)$ Å, ß = 111.43(1)°; $c = 8.804(2)$ Å, $\gamma = 92.66(2)°$; $V = 887.9(3)$ Å^3.

For $Z = 2$ and molecular mass = 343.38, the calculated density is 1.28 g/cm^3. Based on a statistical analysis of intensity distribution and the successful solution and refinement of the structure, the space group was determined to be: P1 (#2). The data were collected at a temperature of 23 ± 1 °C using the ω-2Θ scan technique to a maximum 2Θ value of 121.0°. Omega scans of several intense reflections, made prior to data collection, had an average width at half-height of 0.27° with a take-off angle of 6.0°. Scans of (1.10 + 0.30 tan Θ)° were made at a speed of 32.0°/min (in omega). The weak reflections [$I < 10.0\sigma(I)$] were rescanned (maximum of four scans) and the counts were accumulated to ensure good counting statistics. Stationary background counts were recorded on each side of the reflection. The ratio of peak counting time to background counting time was 2:1. The diameter of the incident beam collimator was 1.0 mm, the crystal to detector distance was 400 mm, and the detector aperture was 9.0 × 13.0 mm (horizontal × vertical). Of the 2737 reflections which were collected, 2588 were unique ($R_{int} = 0.023$). The intensities of three representative reflections were measured after every 150 reflections. No decay correction was applied. The linear absorption coefficient μ for CuK_α radiation is 7.7 cm^{-1}. An empirical absorption correction based on azimuthal scans of several reflections was applied which resulted in transmission factors ranging from 0.90 to 1.00. The data were corrected for Lorentz and polarization effects. The structure was solved by direct methods[31] and expanded using Fourier techniques.[32] The non-hydrogen atoms were refined anisotropically. Hydrogen atoms were included but not refined. The final cycle of full-matrix least-squares refinements was based on 1766 observed reflections [$I > 3.00\sigma(I)$] and 226 variable parameters and converged (largest parameter shift was 0.01 times its ESD) with unweighted and weighted agreement factors of: $R = \Sigma||Fo| - |Fc||/\Sigma|Fo| = 0.043$; $R_\omega = \sqrt{\left[\left(\Sigma\omega(|Fo| - |Fc|)^2/\Sigma\omega Fo^2\right)\right]} = 0.049$. The standard deviation of an observation of unit weight was 1.80. The weighting scheme was based on counting statistics and included a factor ($p = 0.021$) to downweight the intense reflections. Plots of $\Sigma\omega(|Fo| - |Fc|)^2$ versus |Fo|, reflection order in data collection, sin θ/λ and various classes of indices showed no unusual trends. The maximum and minimum peaks on the final difference Fourier map corresponded to 0.17 and −0.25e$^-$/Å^3, respectively.

Neutral atom scattering factors were taken from Cromer and Waber.[33] Anomalous dispersion effects were included in Fcalc,[34] the values for Δf′ and Δf″ were those of Creagh and McAuley.[35] The values for the mass attenuation coefficients are those of Creagh and Hubbell.[36] All calculations were performed using the teXsan[37] crystallographic software package of Molecular Structure Corporation.[38]

7,8-Dihydro-3,10,11,12-tetramethoxydibenz[*b*,*d*]azocin-6(5*H*)-one (9) and 7,8-dihydro-3,10,11,12-tetramethoxydibenz[*c*,*e*]azocin-5(6*H*)-one (10). A solution of 500 mg (1.44 mmol) of the oxime **8** in 25 g of polyphosphoric acid was heated at 65–70 °C for 20 h. The mixture was diluted with 50 mL of water and extracted twice with 30 mL of chloroform. The combined organic layers were dried (Na_2SO_4) and concentrated under reduced pressure. The residue was separated by column chromatography (silica gel, CH_2Cl_2/MeOH 9.9:0.1). Fraction 1 contained 325 mg (65%) of lactam **9** which could be recrystallized from methanol. Fraction 2 contained 36 mg (7%) of lactam **10**.

Compound **9**: colorless crystals, mp 229 °C. UV ($CHCl_3$): λ_{max} (logε) 230 nm (4.58), 252 (4.20). IR (KBr): ν (cm^{-1}) 3168 (NH), 2937 (CH), 1658 (CO). ^{1}H NMR (400 MHz, $CDCl_3$) δ 2.54–2.72 (m, 4H, 7-H, 8-H), 3.53 (s, 3H, OC*H*$_3$), 3.83 (s, 3H, OC*H*$_3$), 3.84 (s, 3H, OC*H*$_3$), 3.85 (s, 3H, OC*H*$_3$), 6.55 (s, 1H, 9-H), 6.75 (d, $^4J = 2.4$ Hz, 1H, 4-H), 6.91 (dd, $^3J = 8.6$ Hz, $^4J = 2.6$ Hz, 1H, 2-H), 7.16 (s, 1H, N*H*), 7.20 (d, $^3J = 8.6$ Hz, 1H, 1-H). ^{13}C NMR (100.5 MHz, $CDCl_3$) δ 29.6 (CH_2, C-8), 35.1 (CH_2, C-7), 55.4 (O*C*H$_3$), 55.9 (O*C*H$_3$), 60.8 (O*C*H$_3$), 60.9 (O*C*H$_3$), 108.3 (CH, C-9), 112.0 (CH, C-4), 113.4 (CH, C-2), 124.2 (C-12a), 128.2 (C-4a), 132.4 (CH, C-1), 134.8 (C-12b*), 136.8 (C-8a*), 141.0 (C-11), 151.1 (C-12*), 153.1 (C-10*), 159.6 (C-3), 174.4 (*C*O). *Assignment not confirmed. MS (70 eV) *m*/*z* (%) 343 (100, M^+), 315 (7), 300 (8). HRMS calcd for $C_{19}H_{21}NO_5$: 343.1419; found 343.1423. $C_{19}H_{21}NO_5$ (343.38) calcd: C 66.46, H 6.16, N 4.08; found C 66.68, H 6.27, N 4.48.

Compound **10**: colorless solid, mp 198 °C. UV ($CHCl_3$): λ_{max} (logε) 228 nm (4.46), 280 (3.68). IR (KBr): ν (cm^{-1}) 3202 (NH), 2925 (CH), 1672 (CO). ^{1}H NMR (500 MHz, CD_2Cl_2) δ 2.69–2.80 (m, 2H, 8-H), 3.25 (m, 1H, 7-H),

3.34 (m, 1H, 7-H), 3.43 (s, 3H, OCH_3), 3.84 (s, 3H, OCH_3), 3.86 (s, 3H, OCH_3), 3.86 (s, 3H, OCH_3), 5.80 (t, ^3J = 5.5 Hz, 1H, NH), 6.51 (s, 1H, 9-H), 6.97 (d, ^4J = 2.75 Hz, 1H, 4-H), 7.01 (dd, ^3J = 8.5 Hz, ^4J = 2.75 Hz, 1H, 2-H), 7.15 (d, ^3J = 8.45 Hz, 1H, 1-H). ^{13}C NMR (125.8 MHz, $CDCl_3$) δ 33.9 (CH_2, C-8), 41.0 (CH_2, C-7), 55.4 (OCH_3), 56.0 (OCH_3), 60.9 (OCH_3), 61.1 (OCH_3), 109.1 (CH, C-9), 111.1 (CH, C-4*), 115.9 (CH, C-2*), 126.2 (C-4a*), 126.4 (C-12a*), 132.0 (C-12b*), 132.2 (CH, C-1), 137.8 (C-8a), 141.2 (C-11), 152.1 (C-12*), 152.8 (C-10*), 159.2 (C-3), 173.9 (C-5). *Assignments not confirmed. MS (70 eV) m/z (%) 343 (100, M^+), 329 (12), 314 (62). HRMS calcd for $C_{19}H_{21}NO_5$: 343.1419, found: 343.1437. $C_{19}H_{21}NO_5$ (343.38): calcd: C 66.46, H 6.16, N 4.08; found C 66.52, H 6.11, N 4.28.

3,11,12,13-Tetramethoxy-8,9-dihydro-dibenzo[*b,d*]tetrazolo[*5,4-h*]azocine (11a). To a solution of 150 mg (0.46 mmol) of ketone **7a** in 2 mL of trifluoroacetic acid 0.09 mL (0.67 mmol) azidotrimethylsilane was added dropwise. The mixture was stirred at room temperature under argon for 24 h. The solvent was evaporated in vacuo and the residue purified by column chromatography (silica gel, ethylacetate/hexane 3:2). Fraction 1 contained 7 mg (5%) of lactam **10**, fraction 2 contained 115 mg of tetrazol **11a** which could be recrystallized from CH_2Cl_2/Et_2O. Fraction 3 yielded 20 mg (13%) of lactam **9**. Colorless crystals, yield 68%; mp 175 °C. UV (CH_2Cl_3): λ_{max} (log ε) 228 nm (4.55), 252 (4.21), 284 (3.86). IR (KBr): ν (cm^{-1}) 2938 (CH), 1615, 1599. ^{1}H NMR (500 MHz, $CDCl_3$) δ 2.81–2.84 (m, 2H, 8-H), 3.22 (m, 1H, 9-H), 3.37 (s, 3H, OCH_3), 3.62 (m, 1H, 9-H), 3.80 (s, 3H, OCH_3), 3.83 (s, 3H, OCH_3), 3.88 (s, 3H, OCH_3), 6.54 (s, 1H, 10-H), 7.05 (d, ^4J = 2.75 Hz, 1H, 4-H), 7.14 (dd, ^3J = 8.6 Hz, ^4J = 2.7 Hz, 1H, 2-H), 7.33 (d, ^3J = 8.7 Hz, 1H, 1-H). ^{13}C NMR (100.5 MHz, $CDCl_3$): δ 25.9 (CH_2, C-9*), 28.4 (CH_2, C-8*), 55.7 (OCH_3), 56.0 (OCH_3), 61.0 (OCH_3), 61.1 (OCH_3), 107.4 (CH, C-10), 111.6 (CH, C-2), 116.8 (CH, C-4), 122.6 (C-13a*), 125.1 (C-13b*), 133.0 (CH, C-1), 133.8 (C-9a*), 134.5 (C-4a*), 141.3 (C-12), 151.4 (C-13), 153.9 (C-11*), 154.1 (C-7a*), 159.6 (C-3). *Assignments not confirmed. MS (70 eV) m/z (%) 368 (44, M^+), 340 (55), 325 (19), 309 (28). HRMS calcd for $C_{19}H_{20}N_4O_4$ (368.39): 368.1484; found: 386.1465.

Crystal structure determination of 11a

To gain single crystals of compound **11a** for X-ray analysis 40 mg of the ligand **11a** were dissolved in boiling methanol (2 mL). The solution was slowly cooled to room temperature and left to stand undisturbed for 24 h, furnishing colorless needles suitable for X-ray crystallographic analysis.

A clear crystal of **11a** having approximate dimension of 0.12 × 0.10 × 0.42 mm was mounted on a glass fiber and investigated on a Rigaku AFC5R diffractometer with graphite monochromated CuK_α radiation and a rotating anode generator (Rigaku). Empirical formula $C_{19}H_{20}N_4O_4$. Cell constants and an orientation matrix for data collection, obtained from a least-squares refinement using the setting angles of 25 carefully centered reflections in the range $71.56 < 2\Theta < 79.96°$ corresponded to a primitive triclinic cell with dimensions: a = 11.023(4) Å, α = 87.554(7)°; b = 21.951(5) Å, ß = 100.689(8)°; c = 7.5977(4) Å, γ = 95.383(9)°; V = 1798(2) Å^3. For Z = 4 and molecular mass 368.39 au, the calculated density is 1.36 g/cm^3. Based on a statistical analysis of intensity distribution and the successful solution and refinement of the structure, the space group was determined to be: P1 (#2). The data were collected at a temperature of 23 ± 1 °C using the Θ ω-2scan technique to a maximum 2Θ value of 120.9°. Omega scans of several intense reflections, made prior to data collection, had an average width at half-height of 0.24° with a take-off angle of 6.0°. Scans of (1.31 + 0.30 tan Θ)° were made at a speed of 32.0°/min (in omega). The weak reflections [$I < 10.0\sigma(I)$] were rescanned (maximum of four scans) and the counts were accumulated to ensure good counting statistics. Stationary background counts were recorded on each side of the reflection. The ratio of peak counting time to background counting time was 2:1. The diameter of the incident beam collimator was 1.0 mm, the crystal to detector distance was 400 mm, and the detector aperture was 9.0 × 13.0 mm (horizontal × vertical). Of the 5000 reflections which were collected, 4889 were unique (R_{int} = 0.035). The intensities of three representative reflection were measured after every 150 reflections. No decay correction was applied. The linear absorption coefficient μ for CuK_α radiation is 8.1 cm. Azimuthal scans of several reflections indicated no need for an absorption correction. The data were corrected for Lorentz and polarization effects. The structure was solved by direct methods[31] and expanded using Fourier techniques.[32] The non-hydrogen atoms were refined anisotropically. Hydrogen atoms were included but not refined. The final cycle of full-matrix least-squares refinements was based on 3733 observed reflections [$I > 3.00\sigma(I)$] and 487 variable parameters and converged (largest parameter shift was 0.01 times its ESD) with unweighted and weighted agreement factors of: $R = \Sigma||Fo| - |Fc||/\Sigma|Fo| = 0.052$; $R_\omega = \sqrt{\left[\left(\Sigma\omega(|Fo| - |Fc|)^2/\Sigma\omega Fo^2\right)\right]} = 0.060$. The standard deviation of an observation of unit weight was 2.15. The weighting scheme was based on counting statistics and included a factor (p = 0.017) to downweight the intense reflections. Plots of $\Sigma\omega(|Fo| - |Fc|)^2$ versus $|Fo|$, reflection order in data collection, $\sin\Theta/\lambda$ and various classes of indices showed no unusual trends. The maximum and minimum peaks on the final difference Fourier map corresponded to 0.22 and −0.27e$^-$/Å^3, respectively.

Neutral atom scattering factors were taken from Cromer and Waber.[33] Anomalous dispersion effects were included in Fcalc,[34] the values for Δf′ and Δf″ were those of Creagh and McAuley.[35] The values for the mass attenuation coefficients are those of Creagh and Hubbell.[36] All calculations were performed using the teXsan[37] crystallographic software package of Molecular Structure Corporation.[38]

11,12,13-Trimethoxy-3-methylthio-8,9-dihydro-dibenzo-[*b,d*]tetrazolo[5,4-*h*]acozine (11b). To a solution of 143 mg (0.42 mmol) of ketone **7b** in 2 mL of trifluoroacetic acid

was added 0.08 mL (0.63 mmol) of azidotrimethylsilane dropwise. The mixture was stirred at room temperature under argon for 4 days. The solvent was evaporated in vacuo and the residue purified by column chromatography (silica gel, ethylacetate/*n*-hexane 1:1) to yield 70 mg (0.18 mmol) of **11b**. The product was recrystallized from chloroform/*n*-hexane to give colorless crystals. Yield 43%; mp 179 °C. UV (CH_2Cl_2): λ_{max} (logε) 230 nm (4.62); 278 nm (4.48). IR (KBr): ν(cm^{-1}) 2939 (CH), 1596, 1486 (C=C), 1143, 1094 (COC). ^{1}H NMR (500 MHz, CD_2Cl_2): δ 2.49 (s, 3H, SCH_3); 2.69–2.79 (m, 2H, 9-H); 3.16 (m, 1H, 8-H_a); 3.35 (s, 3H, OCH_3); 3.54 (m, 1H, 8-H_b); 3.69 (s, 3H, OCH_3); 3.76 (s, 3H, OCH_3); 6.53 (s, 1H, 10-H); 7.26–7.29 (m, 2H, 1-H and 4-H); 7.40 (dd, ^3J = 8.2 Hz, ^4J = 2.0 Hz, 1H, 2-H). ^{13}C NMR (125.8 MHz, CD_2Cl_2): δ 15.2 (SCH_3); 25.8 (CH_2, C-9); 28.3 (CH_2, C-8); 55.9 (OCH_3); 60.7 (OCH_3); 61.0 (OCH_3); 107.5 (CH, C-10); 122.3 (C-13a); 123.5 (CH, C-4*); 127.6 (CH, C-2*); 129.5 (C-13b); 132.4 (CH, C-1), 134.0 (C-9a*); 134.5 (C-4a*); 140.4 (C-3*); 141.3 (C-12*); 151.3 (C-7a); 154.2 (C-13*); 154.3 (C-11*). *Assignments not confirmed. MS (70 eV) *m*/*z* (%) 384 (82; M^+), 359 (10), 356 (100), 341 (19), 325 (27). HRMS calcd for $C_{19}H_{20}N_4O_3S_1$ (384.45): 384.1256; found: 384.1259.

3,10,11,12-Tetramethoxy-7,8-dihydro-6*H*-dibenz[*b*,*d*]azocine (12). To a suspension of 67 mg (1.75 mmol) of lithium aluminium hydride in 20 mL of dry THF was added a solution of 300 mg (0.87 mmol) of lactam **9** in 25 mL of dry pyridine. The mixture was refluxed under argon for 24 h and after cooling to room temperature 15 mL of a saturated aqueous solution of potassium/sodium-tartrate was added slowly. The layers were separated and the aqueous layer was extracted two times with 10 mL of dichloromethane. The combined organic layers were dried (K_2CO_3) and concentrated under reduced pressure. Rapid column chromatography (silica gel, ethyl acetate) yielded fraction 1, containing 158 mg (0.48 mmol) of the oily, yellowish product **12** and a second fraction containing 89 mg (0.26 mmol) of the educt **9**. Yield 55%. IR (film): ν (cm^{-1}) 3408 (NH), 2930 (CH). ^{1}H NMR (500 MHz, $CDCl_3$) δ 1.42 (m, 1H, 7-H), 1.87 (m, 1H, 7-H), 2.62 (m, 1H, 8-H), 2.72 (m, 1H, 8-H), 2.85 (m, 1H, 6-H), 3.23 (m, 1H, 6-H), 3.57 (s, 3H, OCH_3), 3.76 (s, 3H, OCH_3), 3.86 (s, 3H, OCH_3), 3.88 (s, 3H, OCH_3), 6.19 (d, ^4J = 2.4 Hz, 1H, 4-H), 6.33 (dd, ^3J = 8.6 Hz, ^4J = 2.6 Hz, 1H, 2-H), 6.45 (s, 1H, 9-H), 6.91 (d, ^3J = 8.6 Hz, 1H, 1-H). ^{13}C NMR (100.5 MHz, $CDCl_3$) δ 31.0 (CH_2, C-7*), 31.3 (CH_2, C-8*), 42.9 (CH_2, C-6), 55.0 (OCH_3), 55.9 (OCH_3), 60.7 (OCH_3), 61.1 (OCH_3), 102.7 (CH, C-4), 104.2 (CH, C-2), 107.4 (CH, C-9), 113.9 (C-12a*), 127.1 (C-12b*), 134.7 (CH, C-1), 135.5 (C-8a), 140.7 (C-11), 149.1 (C-4a), 151.8 (C-10*), 152.5 (C-12*), 159.5 (C-3). *Assignments not confirmed. MS (70 eV) *m*/*z* (%) 329 (100, M^+), 314 (20), 298 (7). Because of rapid decomposition amine **12** was not further characterized.

1-(3,10,11,12-Tetramethoxy-7,8-dihydro-6*H*-dibenzo[*b*,*d*]azocin-5-yl)-ethanone (13). A solution of 100 mg (0.3 mmol) of the amine **12** and 280 mg (1.5 mmol) of pentafluorophenyl acetate were heated in 3 mL of dry DMF at 80 °C under Argon for 12 h. The solvent was evaporated under reduced pressure and the residue chromatographed on silica gel with ethyl acetate as eluent to yield 104 mg (0.28 mmol) of the product **13** which could be recrystallized from CH_2Cl_2/ether. Colorless crystals, yield 90%, mp 179 °C. UV ($CHCl_3$): λ_{max} (logε) 254 (4.35). IR (KBr): ν (cm^{-1}) 2968 (CH), 1654 (CO). ^{1}H NMR (400 MHz, $CDCl_3$) δ 1.52 (s, 3H, COCH_3), 1.77 (m, 1H, 7-H), 1.92 (m, 1H, 7-H), 2.15 (m, 1H, 8-H), 2.68 (m, 1H, 8-H), 2.81 (m, 1H, 6-H), 3.77 (s, 3H, OCH_3), 3.84 (s, 6H, 2 × OCH_3), 3.87 (s, 3H, OCH_3), 4.59 (m, 1H, 6-H), 6.49 (s, 1H, 9-H), 6.76 (d, ^4J = 2.6 Hz, 1H, 4-H), 6.94 (dd, ^3J = 8.6 Hz, ^4J = 2.6 Hz, 1H, 2-H), 7.25 (d, ^3J = 8.6 Hz, 1H, 1-H). ^{13}C NMR (100.5 MHz, $CDCl_3$) δ 21.6 (COCH_3), 27.6 (CH_2, C-7), 32.8 (CH_2, C-8), 49.3 (CH_2, C-6), 55.4 (OCH_3), 55.8 (OCH_3), 60.3 (OCH_3), 61.3 (OCH_3), 108.1 (CH, C-9), 112.4 (CH, C-4), 113.4 (CH, C-2), 122.9 (C-12a*), 128.7 (C-12b*), 132.6 (CH, C-1), 137.9 (C-8a), 139.9 (C-11), 144.4 (C-4a), 150.8 (C-12*), 153.2 (C-10*), 160.0 (C-3), 169.7 (CO). *Assignments not confirmed. MS (70 eV) *m*/*z* (%) 371 (100, M^+), 356 (3), 328 (3), 312 (4). HRMS calcd for $C_{21}H_{25}NO_5$ (371.43): 371.1732; found: 371.1684.

Crystal structure determination of 13

To gain single crystals of compound **13** for X-ray analysis 8 mg of **13** were dissolved in $CHCl_3$ (0.5 mL) and *n*-hexane (2 mL) was layered carefully down the side of the tube on to the solution. The tube was then corked and left to stand undisturbed for 24 h furnishing colorless crystals suitable for X-ray crystallographic analysis. A clear prism of compound **13** having approximate dimension of 0.15 × 0.10 × 0.20 mm was mounted on a glass fiber and investigated on a Rigaku AFC5R diffractometer with graphite monochromated CuKα radiation and a rotating anode generator (Rigaku). Empirical formula $C_{21}H_{25}NO_5$. Cell constants and an orientation matrix for data collection, obtained from a least-squares refinement using the setting angles of 22 carefully centered reflections in the range $21.14 < 2\Theta < 39.54°$ corresponded to a primitive triclinic cell with dimensions: a = 10.849(2) Å; b = 7.635(4) Å, ß = 99.35(1)°; c = 22.802(2) Å; V = 1864(1) Å^3. For Z = 4 and molecular mass = 371.43 au, the calculated density is 1.32 g/cm^3. The systematic absences of: h01: 1 ≠2n, 0k0: k ≠ 2n uniquely determine the space group to be: $P2_1/c$ (#14). The data were collected at a temperature of 23 ± 1 °C using the ω-2Θ scan technique to a maximum 2Θ value of 120.1°. Omega scans of several intense reflections, made prior to data collection, had an average width at half-height of 0.19° with a take-off angle of 6.0°. Scans of (1.05 + 0.30 tan Θ)° were made at a speed of 16.0°/min (in omega). The weak reflections [$I < 10.0\sigma(I)$] were rescanned (maximum of four scans) and the counts were accumulated to ensure good counting statistics. Stationary background counts were recorded on each side of the reflection. The ratio of peak counting time to background counting time was 2:1. The diameter of the incident beam collimator was 1.0 mm, the crystal to detector distance was 400 mm, and the detector aperture was 9.0 × 13.0 mm (horizontal × vertical). Of the 3200 reflections which were collected, 3021 were unique (R_{int} = 0.058). The intensities of three representative reflection were measured after every 150

reflections. No decay correction was applied. The linear absorption coefficient μ for CuK_α radiation is 7.7 cm·. An empirical absorption correction based on azimuthal scans of several reflections was applied which resulted in transmission factors ranging from 0.91 to 1.00. The data were corrected for Lorentz and polarization effects. The structure was solved by direct methods[39] and expanded using Fourier techniques.[32] The non-hydrogen atoms were refined anisotropically. Hydrogen atoms were included but not refined. The final cycle of full-matrix least-squares refinements was based on 1545 observed reflections [$I > 3.00\sigma(I)$] and 244 variable parameters and converged (largest parameter shift was 0.01 times its ESD) with unweighted and weighted agreement factors of: $R = \Sigma||Fo| - |Fc||/\Sigma|Fo| = 0.055$; $R_\omega = \sqrt{\left[\left(\Sigma\omega(|Fo| - |Fc|)^2/\Sigma\omega Fo^2\right)\right]} = 0.056$. The standard deviation of an observation of unit weight was 1.86. The weighting scheme was based on counting statistics and included a factor ($p = 0.012$) to downweight the intense reflections. Plots of $\Sigma\omega(|Fo| - |Fc|)^2$ versus |Fo|, reflection order in data collection, sin θ/λ and various classes of indices showed no unusual trends. The maximum and minimum peaks on the final difference Fourier map corresponded to 0.28 and $-0.26 e^-/Å^3$, respectively. Neutral atom scattering factors were taken from Cromer and Waber.[33] Anomalous dispersion effects were included in Fcalc,[34] the values for Δf′ and Δf″ were those of Creagh and McAuley.[35] The values for the mass attenuation coefficients are those of Creagh and Hubbell.[36] All calculations were performed using the teXsan[37] crystallographic software package of Molecular Structure Corporation.[38]

3,10,11,12-Tetramethoxy-6,8-dihydro-dibenzo[4,5;6,7]cyclohepta[1,2-*c*]pyrazole (15a) and 3,10,11,12-tetramethoxy-5,8-dihydro-dibenzo[4,5;6,7]cyclohepta[1,2-*c*]pyrazole (15b). To a solution of 157 mg (0.48 mmol) of ketone **7a** in 4 mL of dry DMF was added at 60 °C under an argon atmosphere 0.2 mL (0.96 mmol) of bis(dimethylamino)-*tert*-butoxy-methane (Bredereck's reagent) and the mixture was stirred at 60 °C for 24 h until no more ketone could be detected by TLC. The solvent was evaporated under reduced pressure and the resulting yellow solid was used without further purification. The intermediate enamino ketone was dissolved in 8 mL of methanol and 49 mg (0.48 mmol) of hydrazine dihydrochloride was added. After stirring the mixture for 24 h at room temperature the solvent was evaporated under reduced pressure. Column chromatography of the residue (silica gel, CH_2Cl_2/MeOH 9.8:0.2) yielded 100 mg (0.28 mmol) of pyrazole **15a**/**15b** which could be recrystallized from CH_2Cl_2/*n*-hexane to afford light yellow crystals. Yield 58%, mp 205 °C. UV ($CHCl_3$): λ_{max} (logε) 244 nm (4.46); 270 (4.26). IR (KBr): ν (cm^{-1}) 3365 (NH), 2957 (CH), 1606 (C=N), 1564 (C=C), 1122, 1093 (COC). ^{1}H NMR (500 MHz, $CDCl_3$) δ 3.27 (s, 3H, OCH_3); 3.38 (d, ^2J = 14.2 Hz, 1H, 8-H_a); 3.48 (d, ^2J = 14.2 Hz, 1H, 8-H_b); 3.78 (s, 3H, OCH_3); 3.82 (s, 3H, OCH_3); 3.83 (s, 3H, OCH_3); 6.54 (s, 1H, 9-H); 6.90 (dd, ^3J = 8.7 Hz, ^4J = 2.7 Hz, 1H, 2-H); 7.20 (d, ^4J = 2.7 Hz, 1H, 4-H); 7.34 (s, 1H, 7-H); 7.62 (d, ^3J = 8.7 Hz, 1H, 1-H). ^{13}C NMR (100.5 MHz, $CDCl_3$) δ 30.2 (CH_2, C-8); 55.1 (OCH_3); 55.8 (OCH_3); 60.3 (OCH_3); 61.0 (OCH_3); 106.5 (CH, C-9); 110.7 (CH, C-4); 113.3 (CH, C-2); 121.8 (C-12a*); 124.2 (C-12b*); 125.9 (C-8a*); 134.0 (CH, C-1); 139.2 (C-4a*); 140.8 (C-11); 152.1 (C-10*); 152.4 (C-12*); 158.4 (C-3). *Assignments not confirmed. MS (70 eV) *m*/*z* (%) 352 (100, M^+), 337 (8), 321 (7), 306 (4), 278 (5). HRMS calcd for $C_{20}H_{20}N_2O_4$ (352.39): 352.1423; found: 352.1422.

3,11,12,13-Tetramethoxy-9*H*-5,7-diaza-tribenzo[*a*,*c*,*e*]cyclohepten-6-ylamine (16). To a solution of 170 mg (0.52 mmol) of ketone **7a** in 3 mL of dry DMF was added at 60 °C under an argon atmosphere 0.21 mL (1.04 mmol) of bis(dimethylamino)-*tert*-butoxy-methane (Bredereck's reagent) and the mixture was stirred at 60 °C for 24 h until no more ketone could be detected by TLC. The solvent was evaporated under reduced pressure and the resulting yellow solid was used without further purification. To a freshly prepared sodium ethanolate solution (15 mg of sodium in 5 mL of absolute ethanol) were added 62 mg (0.65 mmol) of guanidine hydrochloride and the mixture was stirred for 30 min at room temperature. Then a solution of the intermediate enamino ketone in dry ethanol was added and the mixture was refluxed under argon for 3.5 h. After cooling to room temperature the light yellow precipitate was separated to give 189 mg (0.50 mmol) of **16** which was recrystallized from ethyl acetate to afford colorless crystals. Yield 96%, mp 272 °C; UV (CF_3CH_2OH) λ_{max} (logε) 226 (4.37), 239 (4.43), 323 (3.54). IR (KBr): ν (cm^{-1}) 3322, 3169 (NH, NH_2), 2934 (CH), 1652 (C=N), 1590, 1546, 1484, 1463 (C=C), 1146, 1121, 1091 (COC). ^{1}H NMR (500 MHz, DMF-d_7): δ 3.24 (d, ^2J = 13.5 Hz, 1H, 9-H_a); 3.43 (s, 3H, OCH_3); 3.58 (d, ^2J = 13.5 Hz, 1H, 9-H_b); 3.74 (s, 3H, OCH_3); 3.86 (s, 3H, OCH_3); 3.89 (s, 3H, OCH_3); 6.50 (s, 2H, NH_2); 6.95 (s, 1H, 10-H); 7.13 (dd, ^3J = 8.7 Hz, ^4J = 2.8 Hz, 1H, 2-H); 7.43 (d, ^4J = 2.8 Hz, 1H, 4-H); 7.61 (d, ^3J = 8.5 Hz, 1H, 1-H); 8.20 (s, 1H, 8-H). ^{13}C NMR (100.5 MHz, DMSO-d_6) δ 33.9 (CH_2, C-9); 55.1 (OCH_3); 55.8 (OCH_3); 60.3 (OCH_3); 60.4 (OCH_3); 106.1 (CH, C-10); 112.9 (CH, C-4); 114.9 (CH, C-2); 122.2 (C-8a*); 123.2 (C-13b*); 127.1 (C-13a*); 132.6 (CH, C-1); 137.6 (C-9a); 138.4 (C-4a*); 140.4 (C-12); 151.5 (C-13*); 152.3 (C-11*); 155.5 (CH, C-8); 157.6 (C-3); 161.7 (C-4b*); 162.9 (C-6*). *Assignments not confirmed. MS (70 eV) *m*/*z* (%) 379 (100, M^+), 364 (12), 349 (5), 348 (6), 306 (3). HRMS calcd for $C_{21}H_{21}N_3O_4$ (379.41): 379.1532, found: 379.1540.

Tubulin binding assay

Calf brain tubulin was purified according to the method of Shelanski,[27] by three cycles of assembly–disassembly and then dissolved in the assembly buffer containing 0.1 M MES, 0.5 mM $MgCl_2$, 2 mM EGTA, and 1 mM GTP pH = 6.6 (the concentration of tubulin was about 2–3 mg/mL). Tubulin assembly was monitored and recorded continuously by turbidimetry at 400 nm in a UV spectrophotometer, equipped with a thermostated cell at 37 °C.[28] We determined for all newly synthesized drugs the IC_{50} values of their concentrations which decreased by 50% the maximum assembly rate of tubulin without drug. The IC_{50} for all compounds were compared to the IC_{50} of deoxypodophyllotoxine, measured the same day under the same conditions.

In vitro characterization of inhibitor-induced effects with respect to the human MCF-7 breast cancer cell line growth

The human MCF-7 breast cancer cell line was obtained from the American Type Culture Collection (ATCC, Rockville, MD, USA). Cell line banking and quality control were performed according to the seed stock concept reviewed by Hay.[40] The MCF-7 cells were maintained in L-glutamine containing Eagle's MEM (Sigma München, Germany) supplemented with $NaHCO_3$ (2.2 g/L) sodium pyruvate (110 mg/L), gentamycin (50 mg/L; Sebio Walchsing, Germany), and 10% fetal calf serum (FCS; Gibco Eggenheim, Germany) using 75 cm^2 culture flasks (Falcon Plastics 3023) in a water-saturated atmosphere (95% air/5% CO_2) at 37 °C. The cell line was weekly passaged after treatment with trypsin (0.05%)/ethylenediaminetetraacetic acid (0.02%; EDTA; Boehringer Mannheim, Germany). Mycoplasma contamination was routinely monitored, and only mycoplasma-free cultures were used.

In vitro testing of (−)-(*aR,7S*)-colchicine (**1**), NCME (**2**) and the newly synthesized allocolchicinoids for antitumor activity was carried out on exponentially dividing human breast cancer cell according to a previously published mictrotiter assay.[30,41] Briefly, in 96-well microtiter plates (Costar), 100 μL of a cell suspension at 500 cells/mL culture medium were plated into each well and incubated at 37 °C for 2–3 days in a humidified atmosphere (5% CO_2). By addition of an adequate volume of a stock solution of the respective compound (solvent: DMF) to the medium the desired test concentration was obtained (max. content of DMF in the medium: 1 ppm). For each test concentration and for the control, which contained the corresponding amount of DMF, 16 wells were used. After the proper incubation time the medium was removed, the cells were fixed with a glutardialdehyde solution and stored at 4 °C. Cell biomass was determined by a crystal violet staining technique as described in refs 40 and 42 The effectiveness of the complexes is expressed as corrected T/C values according to the following equations: Cytostatic effect: T/C_{corr} $[\%]=[T-C_o)/(C-C_o)] \times 100$, where T (test) and C (control) are the optical densities at 578 nm of the crystal violet extract of the cell lawn in the wells (i.e., the chromatin-bound crystal violet extracted with ethanol 70%), and C_o is the density of the cell extract immediately before treatment. Cytocidal effect: $T[\%]=[(T-C_o)/C_o] \times 100$. For automatic estimation of the optical density of the crystal violet extract in the wells a Microplate EL 309 Autoreader was used.

Acknowledgements

This work was generously supported by the Deutsche Forschungsgemeinschaft and the Fonds der Chemischen Industrie. R.B. thanks the DPhG-Stiftung im Stifterverband für die Deutsche Wissenschaft for financial support. We also wish to thank the Merck AG for generous gifts of colchicine, the Bayer AG and Degussa AG for gifts of various chemicals.

References and Notes

1. Brecht, R.; Seitz, G.; Guénard, D.; Thoret, S. *Bioorg. Med. Chem.* **2000**, *8*, 557.
2. Capraro, H.-G.; Brossi, A. In *The Alkaloids;* Brossi, A., Ed.; Academic: New York, 1984; Vol. 23, p 1, and references therein.
3. Boyé, O.; Brossi, A. In *The Alkaloids;* Brossi, A.; Cordell, G.A., Eds.; Academic: New York, 1992; Vol. 41, p 125.
4. Brossi, A. *J. Med. Chem.* **1990**, *33*, 2311.
5. Banwell, M. G. *Pure Appl. Chem.* **1996**, *68*, 539.
6. Hastie, S. B. *Pharm. Ther.* **1991**, *51*, 377.
7. Shi, Q.; Chen, K.; Morris-Natschke, S. L.; Lee, K.-H. *Curr. Pharm. Des.* **1998**, *4*, 219.
8. Brecht, R.; Haenel, F.; Seitz, G. *Liebigs Ann./Recueil* **1997**, 2275, and references cited therein.
9. Kang, G.-J.; Getahun, Z.; Muzaffar, A.; Brossi, A.; Hamel, E. *J. Biol. Chem.* **1990**, *265*, 10255.
10. Bringmann, G.; Walter, R.; Weirich, R. *Angew. Chem., Int. Ed. Engl.* **1990**, *29*, 977.
11. Brossi, A.; Boyé, O.; Muzaffar, A.; Yeh, H. J. C.; Toome, V.; Wegrzynski, B.; George, C. *FEBS. Lett.* **1990**, *262*, 5.
12. Janik, M. E.; Bane, S. L. *Bioorg. Med. Chem.* **2002**, *10*, 1895, and references cited therein.
13. Tomioka, K.; Kubota, Y.; Kawasaki, H.; Koga, K. *Tetrahedron Lett.* **1989**, *30*, 2949.
14. Berg, U.; Bladh, H.; Svensson, C.; Wallin, M. *Bioorg. Med. Chem. Lett.* **1997**, *7*, 2771.
15. Brecht, R. Dissertation, Marburg, April 1999.
16. Guan, J.; Zhu, X.-K.; Brossi, A.; Tachibana, Y.; Bastow, K. F.; Verdier-Pinard, P.; Hamel, E.; McPhail, A. T.; Lee, K.-H. *Collect. Czech. Chem. Commun.* **1999**, *64*, 217.
17. Rapoport, H.; Williams, A. R.; Cisney, M. E. *J. Am. Chem. Soc.* **1951**, *73*, 1414.
18. Kisfaludy, L.; Mohacsi, T.; Low, M.; Drexler, F. *J. Org. Chem.* **1979**, *44*, 654.
19. Imming, P.; Jung, M.-H. *Arch. Pharm. Med. Chem.* **1995**, *328*, 87.
20. Mphahlele, M. J. *J. Chem. Soc., Perkin Trans. 1* **1999**, 3477.
21. Shi, Q.; Chen, K.; Brossi, A.; Verdier-Pinard, P.; Hamal, E.; McPhail, A. T.; Lee, K.-H. *Helv. Chim. Acta* **1998**, *81*, 1023.
22. Bredereck, H.; Effenberger, F.; Simchen, G. *Angew. Chem., Int. Ed. Engl.* **1962**, *1*, 331.
23. Wasserman, H. H.; Ives, J. L. *J. Org. Chem.* **1985**, *50*, 3573 and references cited therein.
24. Bach, N. J.; Kornfeld, E. C.; Jones, N. D.; Chaney, M. O.; Dorman, D. E.; Paschal, J. W.; Clemens, J. A.; Smalstig, E. B. *J. Med. Chem.* **1980**, *23*, 481.
25. Hesse, M.; Meier, H.; Zeeh, B. In *Spektroskopische Methoden in der organischen Chemie*; Georg Thieme: Stuttgart, 1991; Chapter 3, p 183.
26. Marinko, P.; Obreza, A.; Peterlin-Masic, L.; Krbavcic, A.; Kikelj, D. *J. Heterocyclic Chem.* **2000**, *37*, 405.
27. Shelanski, M. L.; Gaskin, F.; Cantor, C. R. *Proc. Natl. Acad. Sci. U.S.A.* **1973**, *70*, 765.
28. Zavala, F.; Guénard, D. *J. Med. Chem.* **1980**, *23*, 546.
29. Boyé, O.; Itoh, Y.; Brossi, A. *Helv. Chim. Acta* **1989**, *72*, 1690.
30. Bernhardt, G.; Reile, H.; Birnböck, H.; Spruß, T.; Schönenberger, H. *J. Cancer Res. Clin. Oncol.* **1992**, *118*, 35.
31. SAPI 91: Hai-Fu, F. In *Structure Analysis Programs with Intelligent Control*; Rigaku Corporation: Tokyo, Japan, 1991.
32. DIRDIF94:Beurskens, P. T.; Admiraal, G.; Beurskens, G.; Bosman, W. P.; de Gelder, R.; Israel, R.; Smits, J. M. M. *The DIRDIF-94 Program System; Technical Report of the*

Crystallography Laboratory; University of Nijmegen: The Netherlands, 1994.
33. Cromer, D. T.; Waber, J. T. *International Tables for X-ray Crystallography*. *Kynoch*; Birmingham: UK, 1974; Vol. IV, Table 2.2A.
34. Ibers, J. A.; Hamilton, W. C. *Acta Crystallogr*. **1964**, *17*, 781.
35. Creagh, D. C.; McAuley, W. J. *International Tables for Crystallography*. *Kluwer Academic*; Boston: MA, 1992; Vol. C, Table 4.2.6.8, p 219.
36. Creagh, D. C.; Hubbell, J. H. *International Tables for Crystallography*; Kluwer Academic: Boston, MA, 1992; Vol. C Table 4.2.4.3, p 200.
37. teXsan: *Crystal Structure Analysis Package*; Molecular Structure Corp., 1985, 1992.
38. Crystallographic data (excluding structure factors) for the structures in this paper have been deposited with the Cambridge Crystallographic Data Centre as supplementary publications nos. CCDC 191524 for compound **8**, 191525 for compound **11a** and 191526 for compound **13**. Copies of the data can be obtained, free of charge, on application to CCDC, 12 Union Road, Cambridge CB2 1EZ, UK (fax: +44-1223-336033, e-mail: deposit@ccdc.cam.ac.uk).
39. SIR92:Altomare, A.; Cascarano, M.; Giacovazzo, C.; Guagliardi, A. *J. Appl. Cryst*. **1993**, *26*, 343.
40. Hay, R. *J. Anal. Biochem*. **1998**, *171*, 225.
41. Reile, H.; Birnböck, H.; Bernhardt, G.; Spruß, T.; Schönenberger, H. *Anal. Biochem*. **1990**, *187*, 262.
42. Gulotti, M.; Pasini, A.; Ugo, R.; Philipeschi, St.; Marmonti, L.; Spreafico, F. *Inorg. Chim. Acta* **1984**, *91*, 223.